AIAA JOURNAL
Vol. 37, No. 3, March 1999

Spurious Numerical Oscillations in Simulation of Supersonic Flows Using Shock-Capturing Schemes

Theodore Kai Lee* and Xiaolin Zhong†
University of California, Los Angeles, Los Angeles, California 90095

The numerical simulation of transitional and turbulent flows in supersonic boundary layers often involves a physical process of a shock–disturbance wave interaction in complex multidimensional flowfields. For such simulations, it is required that there be a high order of accuracy in capturing the shock waves without spurious numerical disturbances. Evaluation of the numerical oscillations generated behind a stationary bow shock by using high-order shock-capturing schemes in computing multidimensional steady supersonic flow over a circular cylinder is carried out. The numerical methods that are studied are the Total Variation Diminishing scheme and the Essentially Non-Oscillatory scheme. Although the general aerodynamic properties are appropriately captured by the shock-capturing schemes, it is shown that there are numerical oscillations in the gradients of the aerodynamic properties in the steady flowfield behind the bow shock, such as for vorticity. These spurious numerical oscillations in the flowfield solution may hinder any attempt at tracking the propagation of physical disturbances behind the shock if unsteady simulations are carried out. They can be significant enough to pollute a flowfield containing small physical disturbances. It is shown that the effects of grid refinement do not reduce the oscillations but rather decrease their wavelength. It is also shown that, by roughly aligning the shock with the grid, the amplitude of these spurious oscillations can be reduced but not eliminated.

Introduction

In numerical simulations of supersonic flowfields, one of the main considerations in using a numerical method is its ability to accurately compute shock waves. Many high-order shock-capturing schemes have been developed to obtain accurate solutions for supersonic flows and have been the main approaches used in practical aerospace applications. Examples of successful shock-capturing numerical schemes include the Total Variation Diminishing (TVD) schemes[1,2] and the Essentially Non-Oscillatory (ENO) schemes.[3] These schemes capture shock waves as part of the numerical solution. The discontinuities of the shock jump are resolved within a few grid cells. Compared with traditional shock-fitting schemes,[4] the shock-capturing schemes have the capability of capturing complex shock interaction patterns without any prior knowledge of the shock shapes. They have been used extensively in flows involving shocks and have been proven to be very effective when used to solve for the general aerodynamic properties of a flow in aerospace applications.

Because of the flexibility of the shock-capturing methods, high-order shock-capturing schemes have previously been extended to the simulation of transitional and turbulent processes in supersonic boundary layers, where it is necessary to accurately capture the interactions between weak physical waves and the shocks. Lee et al.[5] investigated the interaction of isotropic turbulence with a weak shock wave. They found that the turbulence is enhanced during the interaction and that turbulent energy is amplified. Mahesh et al.[6] studied the interaction between a shock wave and a turbulent field of vorticity and entropy fluctuations. They found that the turbulent kinetic energy can be either amplified or suppressed, depending on the correlation between the vorticity and entropy disturbances. Other numerical studies on shock–turbulence interaction using shock-capturing schemes can also be found in Refs. 7–10.

The cited studies were carried out mainly for one-dimensional flows, where the shock is always aligned with the grid. They consisted of only a normal shock, which is aligned with the grid, with a normally incident disturbance. The major difference between a one-dimensional flow and a multidimensional flow is that the shock will usually not be aligned with the grid in a multidimensional flow. Also, any new study of the effects of freestream incident waves would now have to include oblique shock cases, as well as normal shock cases. An example of such a problem is the interaction of freestream disturbances with a bow shock in supersonic flow over a blunt body, where the shape of the curved bow shock is not known in advance. The objective of this paper is to investigate the numerical oscillations in the simulation of steady supersonic flow over a blunt body using shock-capturing schemes without any impinging freestream waves. The previous one-dimensional studies were able to accurately simulate time-dependent flows with disturbances impinging on a normal shock. This was due to the shock being aligned with the grid. Our study is of a steady two-dimensional flow with the numerical generation of disturbances behind the shock due to the shock no longer being aligned with the grid. Any future study of freestream disturbances interacting with a shock over a blunt body cannot be successful if there is already a significant amount of nonphysical numerical oscillation behind the shock. The transmission and generation of disturbances by a freestream wave would be combined with numerical oscillations that exist already, thereby polluting the solution.

To accurately simulate a supersonic flow with small disturbance waves, the shock-capturing method must not generate spurious oscillations that are comparable to the physical disturbance waves. The presence of postshock numerical oscillations in solutions obtained by shock-capturing schemes has recently been studied. Lin[11] found that, for a two-dimensional, slowly moving shock, density oscillations would appear in the postshock region, even though previous studies with a scalar case produced no oscillations at all. Jin and Liu[12] also studied the postshock oscillations found for a slowly moving shock. They note that, because all shock-capturing methods use some degree of artificial viscosity, a smeared shock profile will introduce a spike in the momentum at the discontinuity location. This spike, coupled with the conservation of momentum, will generate spurious oscillations. Arora and Roe[13] point out that the reason for these postshock oscillations is due to the method in which the concept of monotonicity is extended from scalar conservation laws to systems. Methods such as TVD and ENO, which are monotone for scalar cases, fail for systems because they are no longer monotone, even with monotone initial data. Colella and Woodward[14] developed their piecewise parabolic method to provide

Presented as Paper 98-0115 at the AIAA 36th Aerospace Sciences Meeting, Reno, NV, Jan. 12–15, 1998; received March 18, 1998; revision received Oct. 30, 1998; accepted for publication Nov. 8, 1998.

*Graduate Student, Mechanical and Aerospace Engineering Department. Student Member AIAA.

†Associate Professor, Mechanical and Aerospace Engineering Department. E-mail: xiaolin@seas.ucla.edu. Member AIAA.

for a steeper representation of discontinuities. They tested their numerical scheme on a one-dimensional moving shock.

Our specific test case is a supersonic, inviscid, ideal-gas, two-dimensional flow over a circular cylinder. The numerical methods that are studied are the second-order TVD scheme and the third-order ENO scheme. We use these two numerical methods because we are interested solely in the study of the numerical oscillations themselves; therefore, we have chosen two very well-known numerical methods. This study does not involve finding a numerical scheme that has the smallest amount of numerical oscillations. The effects of grid resolution are investigated by a grid refinement study, and the effects of grid alignment are also studied.

Our results concentrate mainly on the vorticity solutions. Because vorticity is the gradient of velocity, it shows the presence of spurious oscillations very clearly, as would the gradient of any other aerodynamic parameter. It is shown that there are spurious numerical oscillations in the vorticity solutions of the steady flowfield. The grid resolution affects the wavelength of the spurious oscillations but has little effect on their amplitude. When the grid resolution is increased, the wavelength of the oscillations decreases.

The effect of grid alignment with the bow shock on the spurious numerical solutions is investigated by using a modified grid so that the shock that has been captured is aligned closely with a grid line. Arora and Roe[13] noted that multidimensional flows involving shock-capturing methods will inevitably result in unwanted spurious oscillations. The effect of aligning the shock with the grid, therefore, is to produce a geometry that is as close to one dimensional as possible in the computational domain. The method of aligning the grid with the shock has recently been used by Carpenter and Casper.[15] Their focus, however, was on the order with which a numerical method captures the shock, rather than the oscillations that are generated behind it. They showed that shock-capturing schemes are all first-order accurate behind the shock. Van Rosendale[16] and Paraschivoiu et al.[17] have used an adaptive grid system to align their grids with the shock. The results show that the effect of aligning the shock with the grid will reduce but not eliminate the amplitude of the numerical oscillations.

Governing Equations and Numerical Methods

The governing equations for inviscid supersonic flows are the Euler equations, the two-dimensional form of which can be written in Cartesian coordinates as follows:

$$\frac{\partial U}{\partial t} + \frac{\partial F}{\partial x} + \frac{\partial G}{\partial y} = 0 \tag{1}$$

where

$$U = \begin{bmatrix} \rho \\ \rho u \\ \rho v \\ e \end{bmatrix}, \qquad F = \begin{bmatrix} \rho u \\ \rho u^2 + p \\ \rho uv \\ ue \end{bmatrix}, \qquad G = \begin{bmatrix} \rho v \\ \rho uv \\ \rho v^2 + p \\ ve \end{bmatrix}$$

In the preceding equations, p is the pressure, ρ is the density, u and v are the horizontal and vertical velocities, $e = [\gamma p/(\gamma - 1)] + [(u^2 + v^2)/2]$ is the total energy per unit volume, and γ is the ratio of specific heats. The gas is assumed to be thermally perfect, with the equation of state given by $p = \rho RT$.

In calculations of supersonic flow over a blunt body, structured body-fitted grids are used. The conservation equations are transformed into curvilinear coordinates associated with the grids before the shock-capturing schemes are applied. We chose to use the ENO and TVD schemes because they are currently among the more popular shock-capturing methods. Highly accurate solutions obtained by a shock-fitting numerical scheme[18] are used to serve as a smooth comparison solution in the evaluation of the solutions obtained by the shock-capturing schemes. The numerical methods used in this paper are briefly introduced in the following sections. Details of the methods can be found in Refs. 1–3.

ENO Scheme

The ENO schemes of Harten et al.[3] were developed by ensuring that the calculated flux was always based on the smoothest stencil. This method of adaptive stencils ensures that the solution will maintain a high order of accuracy up to any discontinuity surface in the flowfields. This is especially important in regions of discontinuity, such as shocks. Therefore, the ENO schemes in flows involving shocks has become highly popular for transient flow simulations. Previous studies of flowfields involving shocks using the ENO schemes include Chiu and Zhong's[19] study of a transient hypersonic flow, as well as that of Mahesh et al.,[6] who studied the interaction of a shock wave with a turbulent shear flow.

The ENO scheme used in this study is the finite difference version of Shu and Osher.[20] This finite difference ENO scheme is chosen because of its simple implementation into multidimensional problems. The finite difference schemes also avoid the costly cell reconstruction procedure of the finite volume ENO scheme, thereby improving the computational efficiency. In this study, the ENO scheme is set to have third-order accuracy.

TVD Scheme

The TVD schemes have been the method of choice for many calculations of aerospace applications since the original concept was introduced by Harten.[1] Whereas many variations on the TVD method have been developed, the basis of all of them remains the same. Previous studies involving the TVD schemes include Yee and Warming's[21] study of a divergent nozzle and a two-dimensional shock reflection problem. The TVD method that is used in this study utilizes the minmod limiter. When considering accuracy, both the TVD and ENO schemes reduce to first-order accuracy at discontinuities.

Shock-Fitting Scheme

The solutions of the shock-capturing schemes are evaluated by comparison with those from a high-order shock-fitting scheme, which are used as smooth comparison solutions. The difference between shock-capturing schemes and shock-fitting schemes is that the shock-fitting scheme uses the shock as its outer boundary, whereas the shock-capturing schemes capture the shock. Because the shock-fitting schemes do not capture the shock, there are no spurious oscillations generated behind the shock. This provides a flowfield free of oscillations with which the ENO and TVD schemes can be compared. The shock-fitting schemes have a disadvantage in that they cannot solve for flowfields that contain complex shock–wave or shock–shock interactions. The shock-capturing schemes, on the other hand, are able to simulate these complex shock interactions. Details of the shock-fitting algorithm can be found in Zhong's[18,22] work for the simulation of a hypersonic flow over a blunt body.

Numerical Results

The accuracy, relative to the shock-fitting solution, and possible spurious numerical oscillations in the solutions of the ENO and TVD shock capturing schemes have been evaluated in this paper for a steady supersonic flow over a circular cylinder. The freestream Mach number is $M_\infty = 4$, and the ratio of specific heats is $\gamma = 1.4$. The computations are carried out on body-fitted grids with uniform spacing in streamwise and wall-normal directions. Figure 1 shows a numerical grid used in the calculations.

To evaluate the relative numerical errors of the shock-capturing schemes, the results of the shock-fitting scheme are used as the smooth comparison solution for the two-dimensional flow. The accuracy of the shock-fitting schemes has been validated in applications to many different steady and transient supersonic flow problems.[18,22] The current Mach 4 flow over a cylinder was previously computed using a spectral shock-fitting scheme by Kopriva et al.[23]

The relative accuracy of the current shock-fitting scheme is further evaluated by computing the same flowfield using four sets of grids: 60×60, 120×120, 150×150, and 240×240 grids. Using the results of the 240×240 grid as a measure, the relative $|l_1|$ errors for pressure behind the shock for an arbitrary line are 3.2×10^{-5} for the 60×60 grid, 6.6×10^{-6} for the 120×120 grid, and 4.2×10^{-6} for the 150×150 grid. The relative $|l_1|$ errors for the vorticity at the same arbitrary line are 8.6×10^{-4} for the 60×60 grid, 1.6×10^{-4}

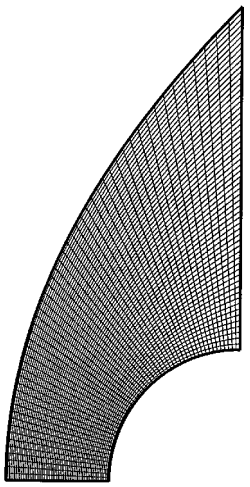

Fig. 1 Grid for the numerical simulation of steady Mach 4 inviscid flow over a two-dimensional circular cylinder.

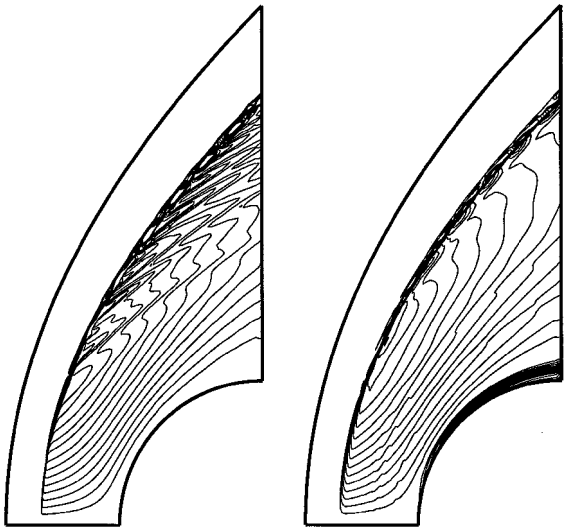

ENO **TVD**

Fig. 2 Vorticity contours for ENO and TVD solutions using a 102 × 120 grid.

for the 120 × 120 grid, and 8.5×10^{-5} for the 150 × 150 grid. These results show that the shock-fitting results are very accurate and can be used for comparison with the shock-capturing schemes.

Spurious Numerical Oscillations Behind the Bow Shock

The shock-capturing schemes are used to compute the same supersonic steady flow over the cylinder. The ENO scheme uses a third-order finite difference ENO scheme of Shu and Osher[20] in space and a second-order explicit Runge–Kutta scheme in time. The TVD scheme uses a second-order minmod limiter in space and a second-order explicit Runge–Kutta scheme in time. The Courant–Friedrichs–Lewy number used in all of the simulations is 0.2.

Although the pressure and other aerodynamic properties do not show the presence of any spurious oscillations, the solutions of the vorticity contours clearly show oscillatory behavior. These oscillations can be easily seen in the vorticity contours of Fig. 2. The size of the grid is 102 × 120. The vorticity oscillations are clearly seen because they are the result of numerical differentiation of the velocity field. We would expect that the gradients of other parameters would contain oscillations as well. The vorticity oscillations, however, are convected along the streamlines. Therefore, we expect them to be present well behind the shock. For most aerodynamic calculations, such numerical oscillations in the vorticity field may not be a problem because the pressure, temperature, and velocity are the main interests of aerodynamic force calculations. However, the quality of the vorticity solutions is critical in transient-wave calculations, where vorticity waves are an important part of the waves generated by shock–disturbance interactions. For the interaction of small freestream waves with a shock, the interaction of any of the three disturbance wave modes (acoustic, entropy, or vorticity) with a shock will generate waves behind the shock involving acoustic waves, entropy waves, and vorticity waves.[24] The contours for the ENO and TVD schemes are not similar in some regions of the flow. This is due to the higher amount of numerical dissipation in the TVD scheme, which acts to smooth out the solution much more than the ENO scheme. The vorticity contours, therefore, seem to be much smoother for the TVD scheme than for the ENO scheme.

The location of these spurious oscillations shows the effect that the numerical grid has on their generation. There appear to be common regions of the flow that are free of oscillations, whereas other areas possess large oscillations. In the region behind the shock near the stagnation line, there are very few spurious oscillations being generated. It is only as the shock becomes more oblique that these oscillations begin to appear and grow in magnitude. This is because, at the stagnation line region, the shock is very well aligned with a grid line. If the shock is aligned with a grid line, it will be sharply captured and, as a result, generate very few or no spurious oscillations. As the shock becomes more oblique, it diverges more from the grid lines, thereby generating larger oscillations. It has been previously reported that these shock-capturing methods show no oscillations for a one-dimensional stationary shock.[13] This is because in a one-dimensional stationary shock, the shock will always be perfectly aligned with the grid.

Effects of Grid Resolution

The effects of grid resolution on the generation of spurious vorticity oscillations are investigated by a grid refinement study using three sets of grids. There is the original grid of 102 × 120 and two additional grids, a coarser 60 × 60 grid and a finer 186 × 240 grid. We have chosen to present the results in terms of distributions along two different lines in the flowfield. The locations of the two lines are shown in Fig. 3. The first line distribution is behind the shock, and the second line distribution is normal to the wall. By comparing the locations of both line distributions with the vorticity contours of Fig. 2, it can be seen that both distributions pass through areas with a small amount of oscillation, as well as a large amount of oscillation.

The vorticity contours are shown in Fig. 2 to have spurious numerical oscillations in the region behind the bow shock for the solutions using the 102 × 120 grid. These oscillations persist when the grids are refined. The vorticity contours for the finer 186 × 240 grid are shown in Fig. 4. The vorticity fields for both the ENO and TVD schemes contain oscillations as grids are refined. The TVD scheme does not show a large difference, again, due to the large amounts of numerical dissipation it possesses. The ENO scheme, however, seems to show that the oscillations become worse as the grid is refined.

The vorticity distribution along the line behind the shock is shown in Fig. 5. It can be seen that the spurious oscillations change as the grid is refined. The line distribution begins close to the stagnation

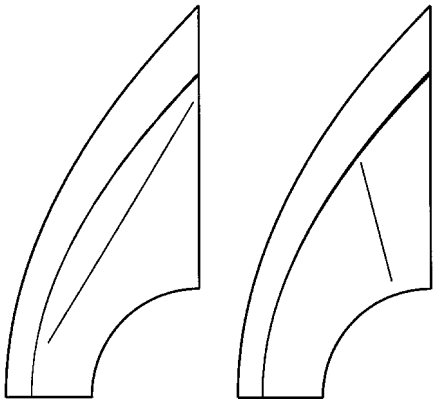

Behind shock **Wall normal**

Fig. 3 Location of the two lines used to plot line distributions of flow variables.

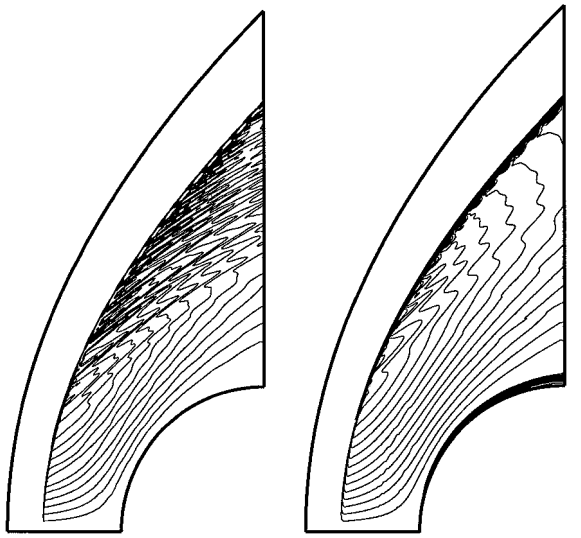

ENO TVD

Fig. 4 Vorticity contours for ENO and TVD solutions using a finer 186 × 240 grid.

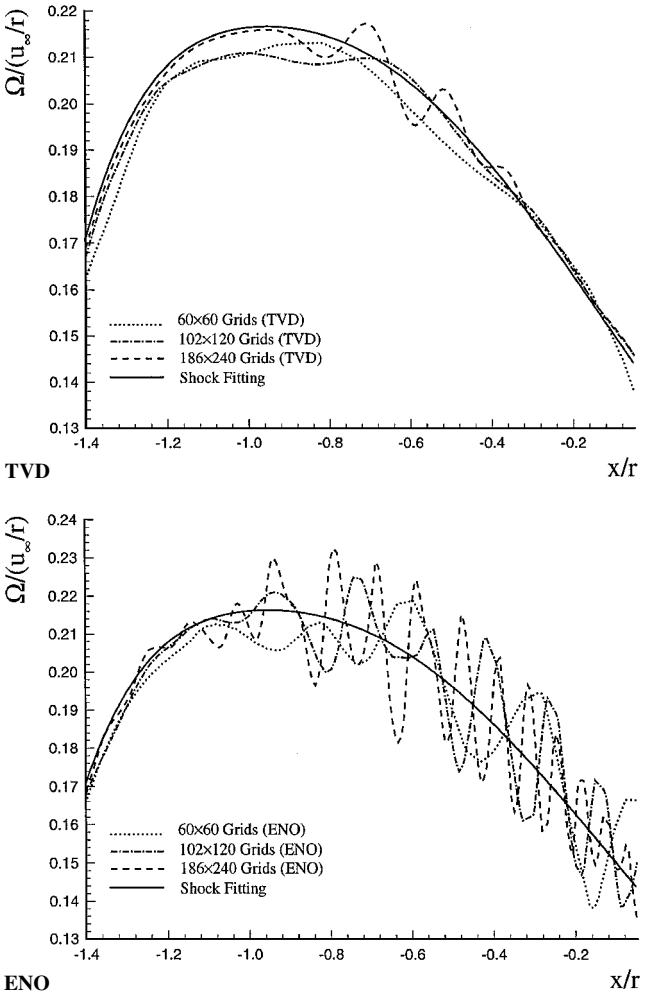

Fig. 5 Vorticity distribution along a straight line behind the shock for the schemes using three sets of grids.

line region, therefore containing no oscillatory behavior. As the line proceeds into the oblique shock region, the oscillations begin to develop. The ENO solution shows that the amplitude of the oscillations is approximately the same with increasing grid resolution. However, it shows that the wavelength decreases with grid resolution. The wavelength is linked to the grid resolution by the size of the grid spacing. The grid spacing become smaller as the grid is refined. The wavelength decreases because of the decreasing grid spacing.

Table 1 Vorticity relative error for nonaligned ENO and TVD grids along straight lines behind the shock and normal to the wall

	Behind the shock		Normal to wall	
Grid	$\|l_1\|$ Errors	$\|l_2\|$ Errors	$\|l_1\|$ Errors	$\|l_2\|$ Errors
ENO 60 × 60	0.044467	0.003787	0.043290	0.003906
ENO 102 × 120	0.039154	0.003521	0.034071	0.003798
ENO 186 × 240	0.039323	0.003558	0.042506	0.004470
TVD 60 × 60	0.026105	0.002111	0.065359	0.007397
TVD 102 × 120	0.017729	0.001538	0.020568	0.002238
TVD 186 × 240	0.012558	0.001108	0.013617	0.001336

The TVD results show that the amount of numerical dissipation in this method greatly reduces the oscillations when compared to the ENO results. However, the fine-grid result still produces more oscillations than the coarse-grid result.

To quantitatively evaluate the relative numerical errors, the $|l_1|$ and $|l_2|$ errors, which are defined by

$$|l_1| = \frac{1}{n}\sum\left(\frac{X - X_{\text{shock-fit}}}{X_{\text{shock-fit}}}\right)$$

$$|l_2| = \frac{1}{n}\left[\sum\left(\frac{X - X_{\text{shock-fit}}}{X_{\text{shock-fit}}}\right)^2\right]^{0.5}$$

for vorticity behind the shock are shown in Table 1 for both numerical schemes. The relative errors are calculated in comparison with the smooth shock-fitting results. The ENO results show no significant changes in the relative error, for either the $|l_1|$ or the $|l_2|$ error. The amplitude of the oscillations is approximately equal in all three grid cases. The effect that the grid has on the oscillation wavelength will not appear in this error analysis. The TVD error results show that the solution seems to improve with finer grid resolution. Even though the finer grid resolution produces a larger amplitude of spurious oscillations, as shown in Fig. 5, the coarse-grid results are not as close to the shock-fitting solution. Therefore, even though the fine-grid relative error is smaller, the amount of oscillation is larger.

The vorticity distributions along a straight line normal to the wall are shown in Fig. 6 for the ENO and TVD schemes. These results support our conclusions involving the vorticity line distributions behind the shock. Again for the ENO case, the oscillations possess approximately the same amplitude while decreasing in wavelength behind the shock with higher grid resolution. The TVD case shows the effects of its numerical dissipation. Again, the $|l_1|$ and $|l_2|$ relative errors are given in Table 1 for the ENO and TVD methods. Similar to the results for relative error behind the shock, the error results for the ENO method stay approximately the same, whereas the TVD results improve with increasing grid resolution. Again, the wavelength of the ENO results will have no effect on the relative error, and the TVD method's numerical dissipation manages to damp out most of the spurious oscillations.

Effects of Grid Alignment

For the vorticity field, Figs. 2 and 4 show that the region near the stagnation line contains very few numerical oscillations, whereas the region behind the oblique shock contains a large amount of oscillation. This is because the grid lines and shock are very well aligned near the stagnation region but not aligned as the shock becomes more oblique. As a possible remedy to the problem of spurious oscillations, it is desired to see how much of an effect adjusting the numerical grid to roughly fit the shock would have on reducing oscillations. The grid shown in Fig. 1 was arbitrarily generated using a quadratic polynomial. By generating a new grid using a fourth-order polynomial, this new grid can be roughly aligned with the shock location that was previously found with the quadratic polynomial grid. The new grid will not, however, be perfectly aligned with the shock. As a result, there are still spurious oscillations being generated by the numerical methods. The goal, however, is to reduce the oscillations enough so that small disturbance waves may be tracked accurately through the flowfield. The new

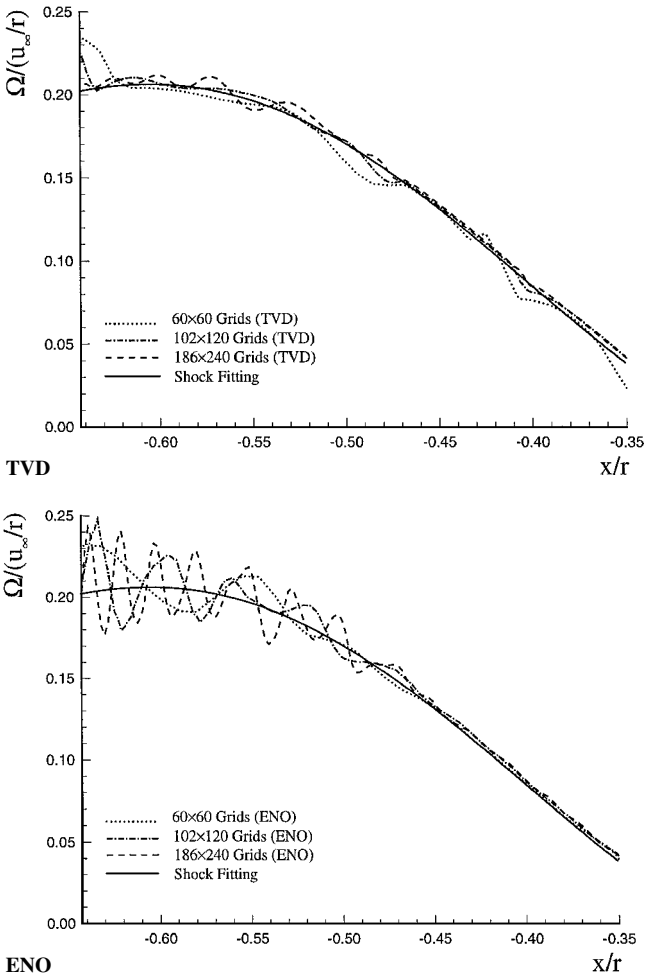

Fig. 6 Vorticity distribution along a straight line normal to the wall for the schemes using three sets of grids.

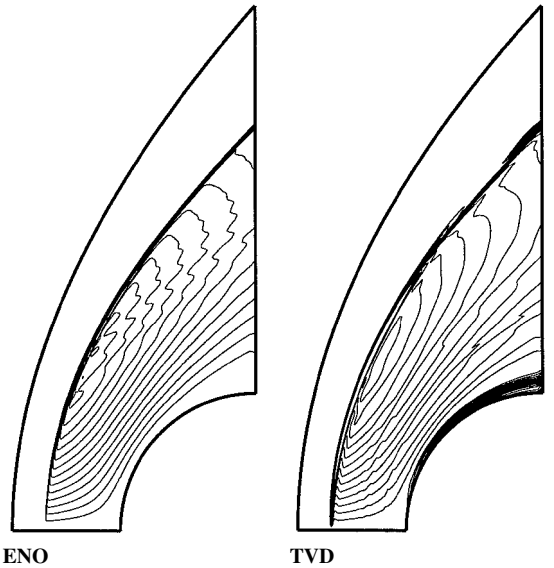

Fig. 7 Vorticity contours for ENO and TVD solutions using a 102 × 120 grid generated so that it is aligned to the bow shock.

grid resolution is still 102 × 120; however, the total size has been slightly altered to account for the alignment of the grid lines with the shock.

The vorticity contours for the ENO and TVD methods, using the grid that is aligned with the shock, are shown in Fig. 7. When these results are compared to those in Fig. 2, the reduction in spurious oscillations is quite significant. Again, there is not much difference between the TVD results, due to the large amount of numerical dissipation. The ENO scheme, however, shows a significant amount of smoothing of the vorticity contour lines. These results support our assertion that the generation of the spurious oscillations is from the crossing of grid lines by discontinuities. Once a discontinuity is roughly aligned with the grid, the results contain much less oscillatory behavior.

Table 2 Vorticity relative error for aligned ENO and TVD grids along straight lines behind the shock and normal to the wall

	Behind the shock		Normal to wall	
Grid	$\|l_1\|$ Errors	$\|l_2\|$ Errors	$\|l_1\|$ Errors	$\|l_2\|$ Errors
ENO normal grid	0.039154	0.003521	0.034071	0.003798
ENO grid aligned	0.015327	0.001352	0.018152	0.001665
TVD normal grid	0.017729	0.001538	0.020568	0.002238
TVD grid aligned	0.017182	0.001479	0.022886	0.002402

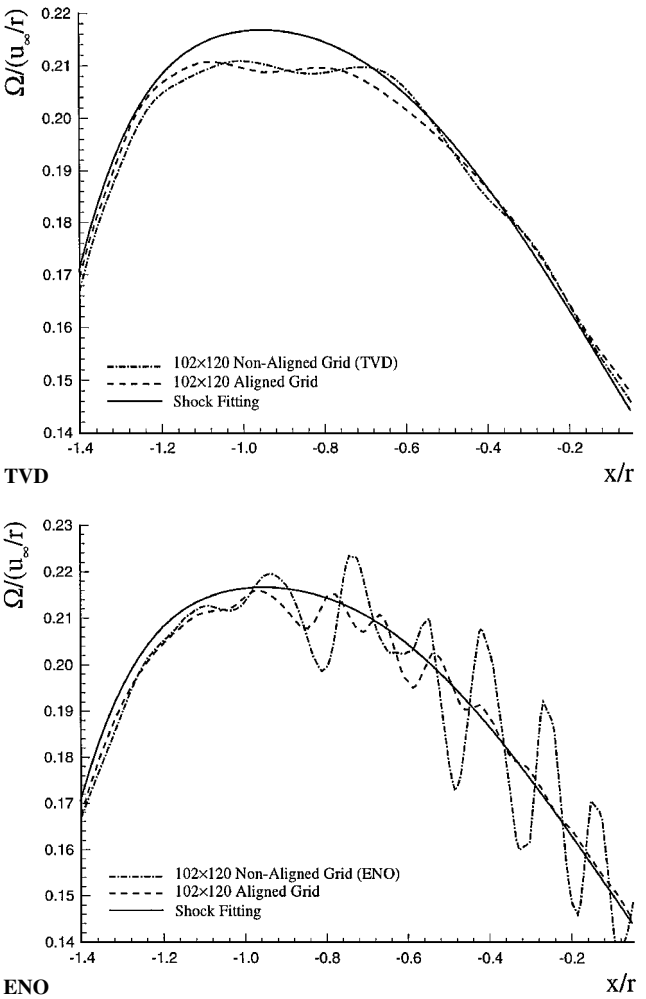

Fig. 8 Vorticity distribution along a straight line behind the shock for the schemes using the aligned grid.

The vorticity distributions along a line behind the shock are shown in Fig. 8 for the ENO and TVD schemes. The ENO method shows a large reduction in the amplitude of the oscillation when used with a grid that is aligned with the shock. The wavelength, however, does not change by a noticeable amount. This supports the assertion that the wavelength is dependent on the grid spacing. Although the two different grids are not identical, they are very similar in size and grid spacing. The TVD method does not show a large improvement, but based on past results, this is expected. The relative errors for the line distributions behind the shock are shown in Table 2 for the ENO and TVD schemes. The ENO method shows significant improvement in both the $|l_1|$ and $|l_2|$ relative errors. The grid that is aligned with the shock manages to reduce the relative errors by over a factor of 2. This is due to the reduction of the

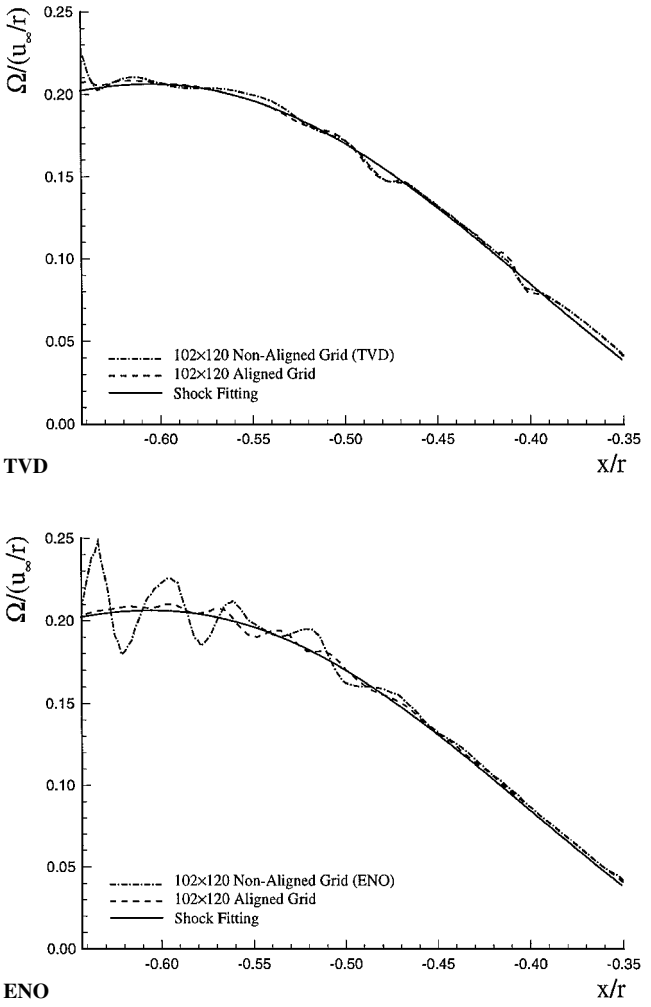

Fig. 9 Vorticity distribution along a straight line normal to the wall for the schemes using the aligned grid.

amplitude of the oscillations. The TVD method did not show the improvement that the ENO method did. The numerical dissipation in the TVD scheme seems to be damping out the spurious oscillations, resulting in relative errors that are almost equal to each other.

The vorticity distributions normal to the wall are shown in Fig. 9 for the ENO and TVD schemes, respectively. Similar to the conclusions found from the results behind the shock, the ENO method generates a spurious oscillation that has a much smaller amplitude when its grid is aligned with the shock. The TVD method shows the effect of numerical damping that is expected. Table 2 shows the relative errors. The ENO method shows the same improvement in relative errors that is found behind the shock. The reduction of the amplitude decreases the $|l_1|$ and $|l_2|$ errors by a large amount. The TVD method follows its pattern of producing errors of roughly the same size, regardless of whether the grid is aligned or not.

Conclusions

The main focus of this paper is to study the generation of spurious numerical oscillations by two shock-capturing numerical schemes as well as the effects of grid resolution and grid alignment. The two shock-capturing methods that were used were the ENO and the TVD numerical schemes. It is found that both grid resolution and grid alignment have large effects on the production of spurious oscillations.

The effect of increasing grid resolution has been shown to decrease the wavelength but not significantly affect the amplitude of spurious oscillations, especially when using the ENO method. Whereas a finer grid will produce a more accurate solution for general aerodynamic values, it could hinder any attempts at tracking small disturbances and capturing small-scale structures in transitional and turbulent flows. The production of spurious oscillations is shown to stem from a discontinuity that crosses over a number of grid lines. When the grids are aligned well with the shock, the amplitude of unwanted oscillations is greatly reduced, especially in the ENO scheme. This is important if we wish to track small disturbances that originate in the freestream and propagate through a shock. If the spurious oscillations are large enough so that a small disturbance wave behind the shock becomes negligible in comparison, then the results obtained will become highly inaccurate. The wavelength, however, is unaffected by the alignment of the grid.

These results show that, although shock-capturing schemes, such as the TVD and ENO schemes, are very successful in aerodynamic calculations for pressure and velocity, caution must be exercised when these methods are applied to the direct numerical simulation of supersonic flow with physical shock disturbance wave interactions. Because any study of a shock–disturbance interaction will involve the tracking of small physical oscillations in the flow, a numerical scheme that has negligible spurious oscillations must be used. It has been shown that two of the popular methods in use today exhibit oscillatory behavior behind the bow shock. Though this behavior can be reduced significantly through an alignment of the shock with the grid, such alignment is not practical in many simulations with moving shocks and complex structures.

Acknowledgments

This research was supported by the U.S. Air Force Office of Scientific Research under Grants F49620-95-1-0405 and F49620-97-1-0030 monitored by Leonidas Sakell.

References

[1]Harten, A., "High Resolution Schemes for Hyperbolic Conservation Laws," *Journal of Computational Physics*, Vol. 49, No. 3, 1983, pp. 357–393.

[2]Chakravarthy, S. R., "A New Class of High Accuracy TVD Schemes for Hyperbolic Conservation Laws," AIAA Paper 85-0363, Jan. 1985.

[3]Harten, A., Engquist, B., Osher, S., and Chakravarthy, S., "Uniformly High Order Accurate Essentially Non-Oscillatory Schemes III," *Journal of Computational Physics*, Vol. 71, No. 2, 1987, pp. 231–303.

[4]Moretti, G., "Computation of Flows with Shocks," *Annual Review of Fluid Mechanics*, Vol. 19, 1986, pp. 313–337.

[5]Lee, S., Lele, S. K., and Moin, P., "Direct Numerical Simulation of Isotropic Turbulence Interacting with a Weak Shock Wave," *Journal of Fluid Mechanics*, Vol. 251, 1993, pp. 533–562.

[6]Mahesh, K., Lele, S. K., and Moin, P., "The Influence of Entropy Fluctuations on the Interaction of Turbulence with a Shock Wave," *Journal of Fluid Mechanics*, Vol. 334, 1997, pp. 353–379.

[7]Mahesh, K., Lee, S., Lele, S. K., and Moin, P., "The Interaction of an Isotropic Field of Acoustic Waves with a Shock Wave," *Journal of Fluid Mechanics*, Vol. 300, 1995, pp. 383–407.

[8]Hannappel, R., and Friedrich, R., "Interaction of Isotropic Turbulence with a Normal Shock Wave," *Applied Scientific Research*, Vol. 51, No. 1–2, 1993, pp. 507–512.

[9]Lee, S., Lele, S. K., and Moin, P., "Interaction of Isotropic Turbulence with a Strong Shock Wave," AIAA Paper 94-0311, Jan. 1994.

[10]Zang, T. A., Hussaini, M. Y., and Bushnell, D. M., "Numerical Computations of Turbulence Amplification in Shock-Wave Interactions," *AIAA Journal*, Vol. 22, No. 1, 1984, pp. 13–21.

[11]Lin, H. C., "Dissipation Additions to Flux-Difference Splitting," *Journal of Computational Physics*, Vol. 117, No. 1, 1995, pp. 20–27.

[12]Jin, S., and Liu, J. G., "The Effects of Numerical Viscosities," *Journal of Computational Physics*, Vol. 126, No. 2, 1996, pp. 373–389.

[13]Arora, M., and Roe, P. L., "On Postshock Oscillations due to Shock Capturing Schemes in Unsteady Flows," *Journal of Computational Physics*, Vol. 130, No. 1, 1997, pp. 25–40.

[14]Colella, P., and Woodward, P. R., "The Piecewise Parabolic Method (PPM) for Gas-Dynamical Simulations," *Journal of Computational Physics*, Vol. 54, No. 1, 1984, pp. 174–201.

[15]Carpenter, M. H., and Casper, J. H., "The Accuracy of Shock Capturing in Two Spatial Dimensions," AIAA Paper 97-2107, June 1997.

[16]Van Rosendale, J., "Floating Shock Fitting via Lagrangian Adaptive Meshes," AIAA Paper 95-1721, June 1995.

[17]Paraschivoiu, M., Trépanier, J. Y., Reggio, M., and Camarero, R., "A Conservative Dynamic Discontinuity Tracking Algorithm for the Euler Equations," AIAA Paper 94-0081, Jan. 1994.

[18]Zhong, X., "Direct Numerical Simulation of Hypersonic Boundary-Layer Transition over Blunt Leading Edges, Part I: A New Numerical Method and Validation," AIAA Paper 97-0755, Jan. 1997.

[19]Chiu, C., and Zhong, X., "Numerical Simulation of Transient Hypersonic Flow Using the Essentially Nonoscillatory Schemes," *AIAA Journal*, Vol. 34, No. 4, 1995, pp. 655–661.

[20]Shu, C. W., and Osher, S., "Efficient Implementation of Essentially Non-Oscillatory Shock-Capturing Schemes," *Journal of Computational Physics*, Vol. 77, No. 2, 1988, pp. 439–471.

[21]Yee, H. C., and Warming, R. F., "Implicit Total Variation Diminishing (TVD) Schemes for Steady-State Calculations," *Journal of Computational Physics*, Vol. 57, No. 3, 1985, pp. 327–360.

[22]Zhong, X., "Direct Numerical Simulation of Hypersonic Boundary-Layer Transition over Blunt Leading Edges, Part II: Receptivity to Sound," AIAA Paper 97-0756, Jan. 1997.

[23]Kopriva, D. A., Zang, T. A., and Hussaini, M. Y., "Spectral Methods for the Euler Equations: The Blunt Body Problem Revisited," *AIAA Journal*, Vol. 29, No. 9, 1991, pp. 1458–1462.

[24]McKenzie, J. F., and Westphal, K. O., "Interaction of Linear Waves with Oblique Shock Waves," *Physics of Fluids*, Vol. 11, No. 11, 1968, pp. 2350–2362.

K. Kailasanath
Associate Editor